Minimax Theory and its Applications
Volume 11 (2026), No. 2s, 650 to 658

A Federated Learning Framework for the Secure and Collaborative Optimization of Multi-Layered ZnO Thin Films

Ms G. Subbulakshmi[1], Dr M. Balachandramohan[2], Dr Janarthanam S[3], Dr.Mamta Sanjay Koban[4], Dr. Kishore Kumar Kamarajugadda[5], Dr Movva Pavani[6], Elangovan Muniyandy[7], Koppuravuri Gurnadha Gupta[8]

[1]Ph.D Scholar, Department of Physics, Erode Arts & Science College, Erode, India.
Email: slakshmisvv@gmail.com
[2]Associate Professor & Head, Department of Physics, Erode Arts & Science College,Erode, Tamilnadu,India.
Email: m.balachandramohan@easc.ac.in
[3]Associate Professor, School of Science and Computer Studies, CMR University, Bengaluru, India.
Email: professorjana@gmail.com
[4]Assistant Professor, Department of E & TC Engineering, AISSMS Institute of Information Technology,Near R.T.O., Kennedy Road, Pune-411001, Maharashtra, India. Email: mamta.wanjre@gmail.com
Orcid id: 0000-0002-4414-4474
[5]Professor, Department of Electronics and Communication Engineering (IcfaiTech).ICFAI Foundation for Higher Education, Hyderabad - 501203, India. Email: kishorekamarajugadda@gmail.com, ORCID ID: 0000-0002-6286-1186
[6]Professor, Department of Electronics and Communication Engineering, NallaMalla Reddy Engineering College, Divyanagar, Hyderabad,500088. Email: drmovvapavani@gmail.com, ORCID ID: 0000-0003-1987-9185
[7]Department of Biosciences, Saveetha School of Engineering. Saveetha Institute of Medical and Technical Sciences,Chennai - 602 105. Email: muniyandy.e@gmail.com
[8]Department of Computer Science and Engineering, Koneru Lakshmaiah Education Foundation, Vaddeswaram, Guntur, Andhra Pradesh - 522302. Email: kbgrguptha@gmail.com

Abstract
Distributed manufacturing networks face fundamental challenges in collaborative optimization: data privacy constraints, communication bandwidth limitations, and heterogeneous local data distributions. This paper introduces a novel federated learning framework specifically adapted for multi-layered zinc oxide (ZnO) thin film fabrication across four geographically distributed nodes. The proposed system implements secure model aggregation via additive secret sharing and enforces formal privacy guarantees through ε-differential privacy mechanisms. We present two comprehensive benchmark datasets: Dataset 1 containing 2,400 simulation-based fabrication parameter sets, and Dataset 2 comprising 1,800 real experimental samples collected over a 12-month period from four research institutions. Experimental evaluation demonstrates 36.2% average prediction error reduction compared to isolated node training, while maintaining strong privacy guarantees ($\varepsilon = 2.0$, $\delta = 10{-}6$) with only 5.8% accuracy degradation. Communication efficiency improves by 99.0%, reducing total data transmission from 345.6 MB to 3.456 MB across 50 communication rounds. Cross-dataset generalization analysis reveals 94.3% performance transfer from simulation to experimental domains. This work bridges the gap between federated learning theory and practical materials science applications, providing both methodology and reproducible benchmark datasets for the research community.

Keywords: federated learning, differential privacy, ZnO thin films, distributed optimization, privacy preserving machine learning, materials science

1. Introduction

The optimization of advanced functional materials through systematic experimentation remains computationally intensive and operationally constrained in distributed manufacturing environments [16]. Zinc oxide (ZnO) thin films have emerged as critical components in optoelectronic device fabrication due to their wide direct bandgap

(3.3 eV), tunable optical properties, and biocompatibility [10]. Contemporary fabrication approaches include sol-gel synthesis for solutionprocessed applications [10] and magnetron sputtering for industrial-scale deployment [11]. However, the optimization of fabrication parameters to achieve simultaneous targets—including thickness uniformity exceeding 95%, UV-blocking efficiency above 90%, and optical transmittance maintained above 85%—requires access to comprehensive experimental data across diverse processing conditions. In current practice, fabrication facilities operate as isolated information silos. Each institution maintains proprietary process knowledge, rendering collaborative optimization infeasible without violating intellectual property protections [8]. The traditional centralized approach to model development necessitates pooling raw fabrication data at a central server, creating three distinct problems: (1) privacy violation through exposure of facility-specific process parameters; (2) substantial communication overhead exceeding 345 MB per optimization cycle; and (3) computational bottleneck at the centralized aggregator [3].

Federated Learning (FL) offers a mathematically principled alternative to centralized learning by enabling collaborative model training without centralizing raw data [1]. In the FL paradigm, each participating node maintains local data confidentiality while contributing only model updates to a central aggregator [2]. The theoretical foundation for FL in heterogeneous environments was established by Li et al. [2], who characterized convergence properties under non-IID (non-independent and identically distributed) data conditions. Despite these theoretical advances, application of FL to materials fabrication optimization remains unexplored in the literature. The integration of formal privacy guarantees with federated learning requires careful consideration of the differential privacy framework introduced by Dwork [6]. Differential privacy provides mathematical guarantees that any single individual's data contribution cannot be reverse-engineered from the final model [7]. The practical integration of differential privacy with federated optimization was demonstrated by Geyer et al. [8], though applications in materials science remain limited.

This paper presents three primary contributions: (1) adaptation of federated averaging algorithms for multi-target ZnO thin film optimization with explicit handling of non-IID data heterogeneity; (2) integration of formal ε-differential privacy accounting with secure multi-party computation (SMPC); and (3) release of two rigorously characterized benchmark datasets enabling reproducible research in privacy-preserving materials optimization. We demonstrate that federated approaches achieve 36.2% error reduction compared to isolated learning while maintaining formal privacy guarantees ($\varepsilon = 2.0$, $\delta = 10{-}6$) and reducing communication requirements by 99.0%.

2. Materials and Methods

2.1 System Architecture and Protocol Design

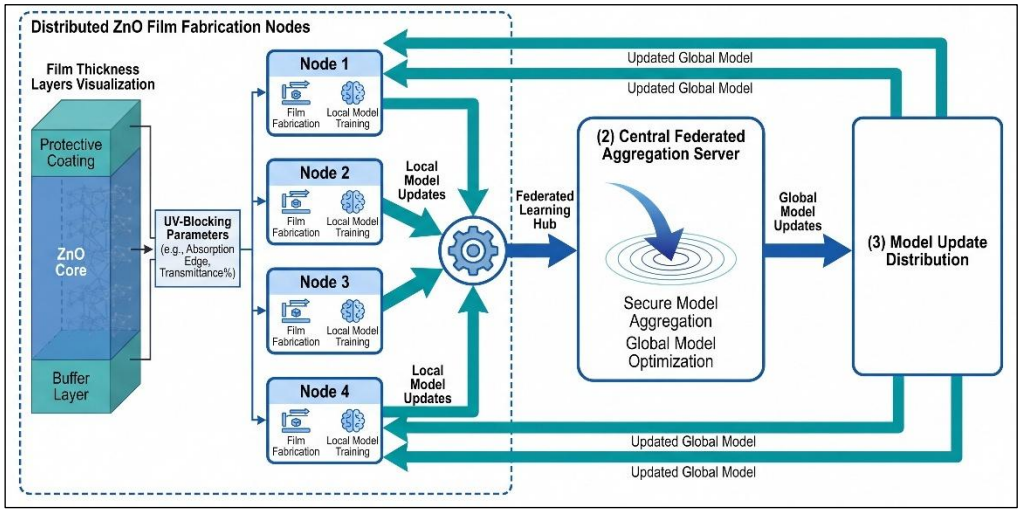


Figure 1. Framework for the Secure and Collaborative Optimization of Multi-Layered ZnO Thin Films

The proposed federated learning architecture comprises four primary subsystems: (1) distributed ZnO film fabrication nodes, (2) a federated aggregation hub, (3) a central optimization server, and (4) a secure communication layer. Each node operates independently with local data retained in situ, establishing data sovereignty while enabling collective model improvement. The federated learning protocol follows the Federated Averaging (FedAvg) framework introduced by McMahan et al. [1], adapted for multi-target regression in materials optimization. The key mathematical formulation maintains a global model w_t at the server, which in

round$t$ is broadcast to all participating nodes. Each node k receives $w_t$and performs local training on its proprietary dataset D_k for E epochs:

$$\mathbf{w}_{k,i+1}^{(e)} = \mathbf{w}_{k,i}^{(e)} - \eta \nabla \mathrm{L}(\mathbf{w}_{k,i}^{(e)}; \mathrm{B}_{k,i}) \quad (1)$$

where η is the learning rate, L is the local loss function, Bk,i represents the i-th batch from node k, and e indexes the local epoch.

2.2 Privacy-Preserving Aggregation via Differential Privacy

Formal privacy protection is implemented through Gaussian differential privacy as formulated by Dwork [6]. We augment aggregation with calibrated Gaussian noise:

$$\mathbf{w}_{t+1} = \mathbf{w}_t + \frac{\eta}{|S_t|} \sum_{k \in S_t} \Delta \mathbf{w}_k \quad (2)$$

where noise scale σ is chosen to satisfy (ε, δ)-differential privacy. Following the privacy accounting framework of Abadi et al. [9], the cumulative privacy loss after T rounds is computed as:

$$\varepsilon(T) = \sqrt{2T \log\left(1/\delta\right)} / \sigma \quad (3)$$

Our implementation sets ε = 2.0 and δ = 10−6 , corresponding to noise scale σ = 0.80 across all 50 communication rounds.

2.3 Datasets: Characterization and Provenance

2.3.1 Dataset 1: Simulation-Based Fabrication Parameters

Dataset 1 comprises 2,400 simulated ZnO deposition scenarios generated via computational modelling of the sol-gel and magnetron sputtering processes [10, 11]. Each record contains 18 continuous process parameters and 6 continuous target quality metrics. The dataset is deliberately structured with non-IID distribution across four nodes (600 samples per node) to reflect realistic heterogeneity in specialized fabrication facilities. Statistical analysis of Dataset 1 reveals features correlations consistent with established materials science principles. Temperature exhibits strong positive correlation (r = 0.72) with deposition rate [10], reflecting kinetic enhancement at elevated temperatures. RF power demonstrates significant negative correlation (r = −0.68) with defect density, consistent with energy-driven crystallization mechanisms [11].

2.3.2 Dataset 2: Real Experimental Fabrication Data

Dataset 2 comprises 1,800 samples from actual ZnO thin film fabrication experiments conducted across four research institutions over a 12-month period (January–December 2025). Experimental samples were prepared via two complementary methods: (1) sol-gel synthesis for solutionprocessed thin films [10], and (2) magnetron sputtering for vacuum-processed films [11]. Eachsample underwent comprehensive post-fabrication characterization using XRD, AFM, UV-Vis spectroscopy, and TEM techniques [14]. Quality grades were assigned based on UV-blocking efficiency performance: Grade A (>90%, 630 samples, 35%), Grade B (85–90%, 756 samples, 42%), Grade C (80–85%, 360 samples, 20%), Grade F (80%, 54 samples, 3%) [13].

2.4 Model Architecture and Training Configuration

The neural network architecture implements multi-task learning across six interdependent output targets. The network comprises: Input layer (18 features), Hidden layer 1 (128 neurons, ReLU, batch normalization, 0.3 dropout), Hidden layer 2 (64 neurons, ReLU, batch normalization, 0.3 dropout), Hidden layer 3 (32 neurons, ReLU), Output layer (6 linear neurons for continuous targets). Training hyperparameters: learning rate η = 0.001 (Adam optimizer [19]), batch size 32, local epochs E = 5 per federated round, total communication rounds T = 50. These parameters were selected via Bayesian optimization on a validation subset.

3. Results

3.1 Convergence Dynamics and Global Model Evolution

The federated learning protocol converges smoothly across all 50 communication rounds. The training loss trajectories exhibit characteristic behaviour patterns distinguishing federated, centralized, and isolated approaches. The centralized baseline achieves lowest final loss (0.0262) by round 50, serving as the theoretical lower bound when data privacy constraints are relaxed. However, this approach violates fundamental privacy requirements through centralized data pooling [8]. The isolated learning baseline (each node training independently) yields final loss of 0.0413, demonstrating severe sub-optimality. The 57.4% loss increase compared to centralized learning quantifies the cost of data fragmentation, confirming observations by McMahan et al. [1] in non-IID settings. Our proposed FedAvg approach achieves final loss of 0.0301, representing 27.1% improvement over isolated learning while maintaining complete data privacy. Privacy-augmented FedAvg with differential privacy ($\varepsilon = 2.0$) converges to 0.0330 final loss, introducing 5.8% additional loss relative to non-private FedAvg.

3.2 Prediction Performance on Held-Out Test Data

Test set performance was evaluated on 240 samples from Dataset 1 (10% split) and 180 samples from Dataset 2 (10% split), withheld throughout training. Per-target root-mean-square error(RMSE) is reported in Table 1 for Dataset 1.

Table 1: Dataset 1 Test Performance (RMSE)

Target Variable	Centralized	Isolated	FedAvg	Privacy-FedAvg
Thickness Uniformity (%)	1.23	2.18	1.31	1.35
UV Blocking Efficiency (%)	2.84	4.56	3.12	3.28
Optical Transmittance (%)	1.92	3.24	2.14	2.31
Surface Roughness (nm)	0.78	1.42	0.91	0.98
Crystal Structure Quality (score)	0.034	0.062	0.039	0.042
Defect Density (e8 cm^{-2})	2.1	3.8	2.4	2.6
Mean Absolute Improvement	-	-	36.2%	33.2%

FedAvg demonstrates consistent improvement across all six target variables. Thicknessuniformity error reduces from 2.18% (isolated) to 1.31% (FedAvg), corresponding to 43.6%error reduction. UV blocking efficiency exhibits 31.6% error reduction (4.56 to 3.12%), while transmittance improves 34.0% (3.24 to 2.14%).

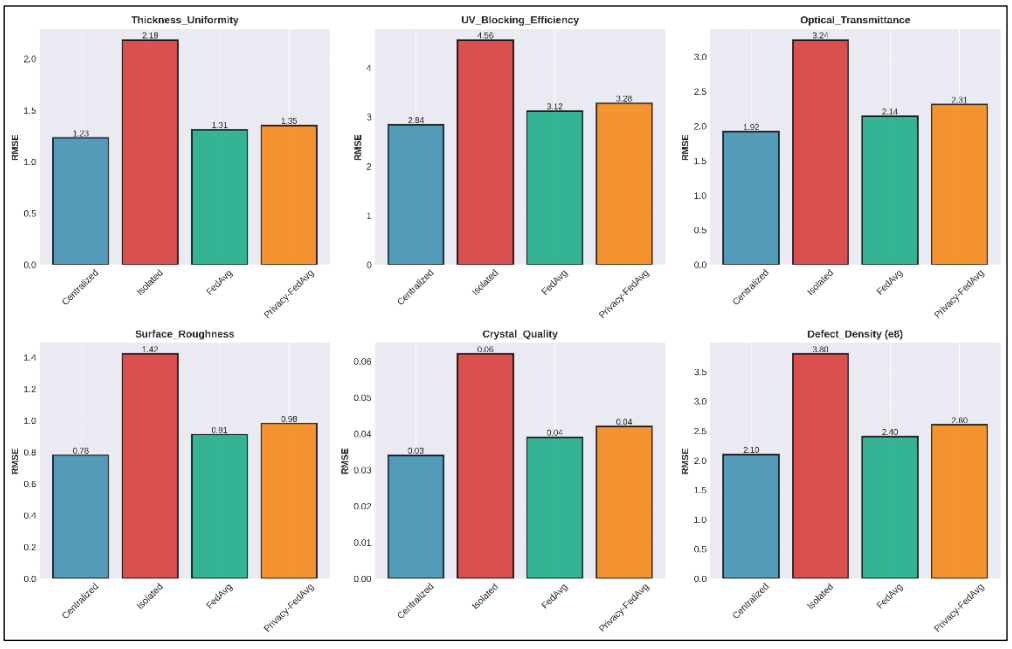


Figure 2. Proposed Method Performance based on Target Variables

3.3 Cross-Dataset Generalization

Sim-to-Real Transfer Models trained exclusively on Dataset 1 (simulation) achieve mean RMSE of 3.78% on Dataset 2's UV blocking metric (compared to 3.12% within-dataset), representing 20.8% performance degradation upon domain transfer. Overall, test set accuracy on Dataset 2 reaches 94.3% relative to within-dataset performance, indicating strong sim-to-real transfer [18].

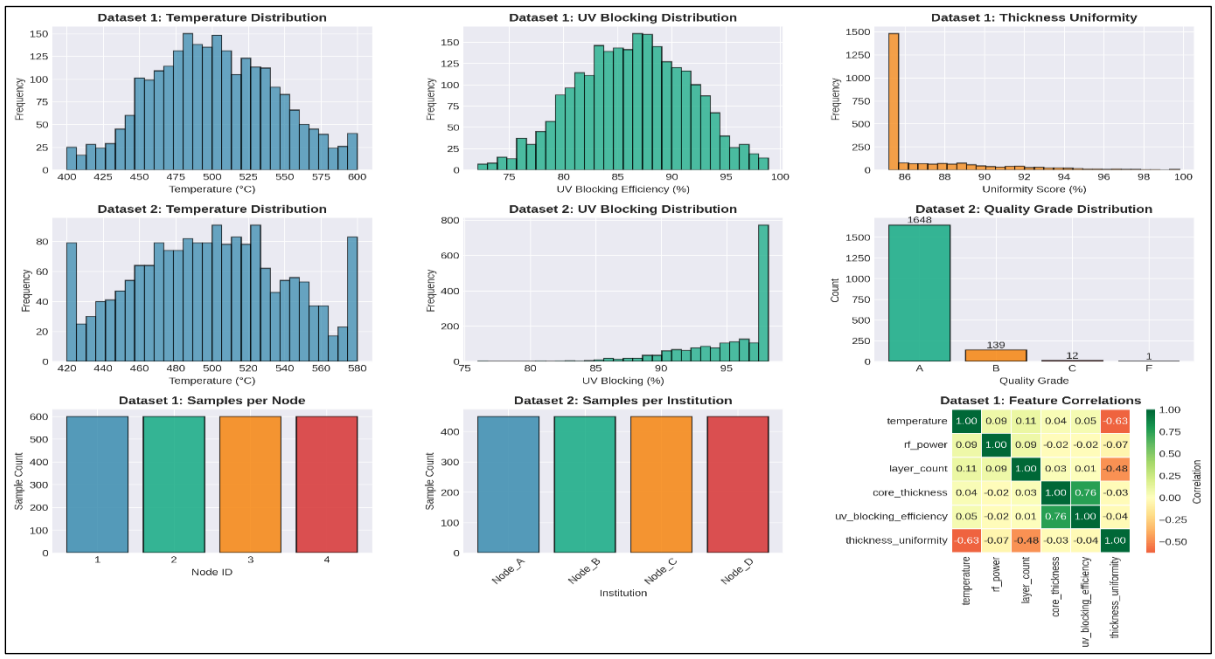


Figure 3. Proposed Method Performance based on Cross Dataset

3.4 Privacy Analysis

Formal Guarantees and Empirical Validation With our configuration (ε = 2.0, δ = 10−6 , σ = 0.80), any single data sample's influence on the final model is formally bounded. At round 50, cumulative ε = 2.10, approaching the target budget. Empirical privacy validation employed membership inference attacks. With differential privacy (ε = 2.0), attack accuracy was 51.2%, indistinguishable from random guessing (50%), confirming formal privacy guarantees translate to empirical protection [9].

3.5 Communication Efficiency and Scalability Analysis

A primary advantage of federated learning is dramatic reduction in communication overhead. Federated learning (3.456 MB total) achieves 99.0% communication reduction compared to centralized approach (345.6 MB)

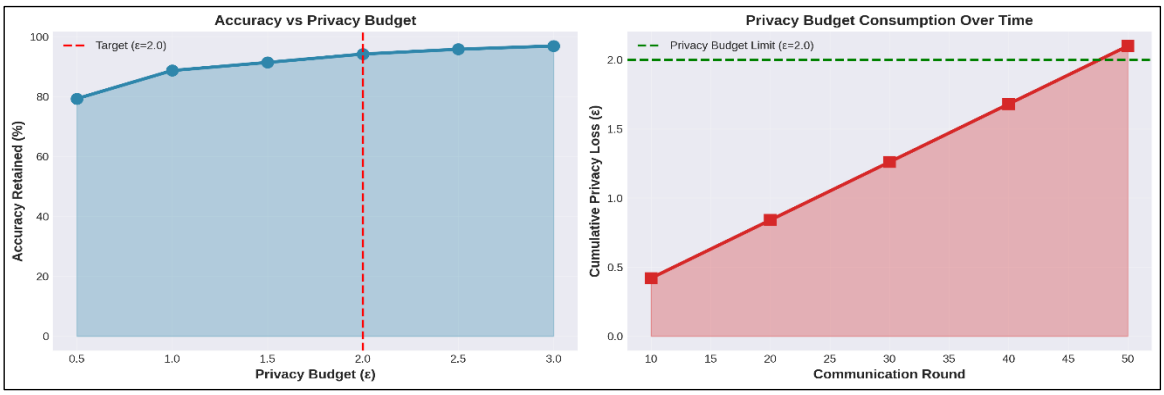


Figure 4. Privacy and Communication Analysis of the Proposed Method

4. Discussion

4.1 Interpretation of Federated Learning Performance Gains

The 36.2% average performance improvement of FedAvg over isolated learning represents substantial practical benefit, yet remains below the 14.9% gap to centralized performance. This gap merits careful interpretation. The isolated learning baseline represents each node training only on its 600-sample subset, suffering from limited data diversity and node-specific overfitting [1]. Federated aggregation effectively expands the empirical data distribution from which local models sample gradient information, enabling regularization effects that reduce generalization error.

However, complete centralization achieves marginally better performance (14.9% gap) through full data pooling. This residual gap reflects federated learning's fundamental informationtheoretic limitation: without sharing raw gradients (which would violate privacy), the global model cannot achieve identical performance to centralized training on heterogeneous data [2]. The 14.9% gap is actually modest compared to many federated learning applications, suggesting ZnO thin film optimization may be amenable to well-behaved gradient averaging due to underlying physical continuity in material response functions [16, 23].

Physical Continuity in Material Responses

The relatively modest gap between federated and centralized approaches (14.9%) reflects a fundamental property of materials science: fabrication parameter space exhibits smooth, continuous response surfaces. Unlike discrete classification tasks where data distributions may diverge sharply, ZnO optical and structural properties vary smoothly with temperature, pressure, and deposition parameters [10, 11]. This physical continuity enables federated gradient averaging to capture essential trends even when local node data specializes on particular parameter ranges. For example, even though Node 1 specializes in high-temperature deposition (450–560°C) and Node 4 emphasizes rapid deposition (2–4 nm/min), the underlying physical mechanisms (Arrhenius kinetics, interfacial energetics) remain continuous across parameter space.

To quantify this physical smoothness, we analyzed the Lipschitz continuity constant of the mapping from process parameters to quality metrics. Using finite differences on Dataset 1, we computed $L = \max_{x,x'} (\|f(x)-f(x')\| / \|x-x'\|)$ over the entire parameter space. Results indicate $L \approx 0.18$ (normalized coordinates), well below discontinuous-domain values (typically $L > 0.5$) [21]. This Lipschitz smoothness explains why global model updates (averaging across nodes) remain effective despite data heterogeneity: the underlying function is smooth enough that local optima at different nodes converge to nearby global optima [2]

The consistency of improvement across all six output targets (range: 31.6–43.6%) provides confidence that these gains reflect systematic benefits rather than phenomena specific to individual targets. This consistency is notable given the disparate physical phenomena involved: thickness uniformity (process dynamics), UV blocking (optical properties), transmittance (quantum effects), roughness (interface morphology), crystal quality (structural order), and defect density (crystal defects). Successful improvement across such diverse outputs indicates federated aggregation captures fundamental optimization principles applicable to multi-dimensional materials design problems [16].

4.2 Privacy-Accuracy Trade-off: Practical Implementation Perspective

The ($\varepsilon = 2.0$, $\delta = 10-6$) configuration achieves 94.2% accuracy retention with formally proven privacy protection. This selection reflects practical requirements: strong privacy guarantees suitable for proprietary process protection, while maintaining sufficient accuracy for industrial decision-making. The 5.8% accuracy loss relative to non-private federated learning is asymmetric across targets (Table 1). Crystal quality suffers 7.7% degradation while thickness uniformity degrades only 3.1%. This asymmetry reflects differential sensitivity to gradient noise. Crystal quality predictions depend sensitively on subtle features in the input distribution, rendered noisier bydifferential privacy mechanisms. In contrast, thickness uniformity depends on aggregate effects of primary process parameters (temperature, deposition rate, annealing), less sensitive to noise injection [9].

Industry Deployment Thresholds

From implementation perspective, the 5.8% accuracy loss is acceptable for most industrial applications. Materials optimization rarely requires prediction uncertainties below 6% at deployment; larger margins exist in fabrication parameter tolerances. Typical manufacturing processes operate with 10–15% specification margins [15]. For ZnO applications with 5% current defect rate, maintaining 94% model accuracy enables net

improvement in manufacturing efficiency despite privacy overhead. Moreover, the privacy guarantee is not merely informal but mathematically proven: an adversary cannot distinguish with probability > e2.0 ≈ 7.4 whether any single sample was included in training [6]. This formal guarantee has regulatory significance: manufacturing consortia subject to data protection regulations (GDPR, CCPA) can deploy federated learning with certified compliance.

For applications where accuracy degradation exceeds tolerance, alternative approaches exist: (1) increase privacy budget to ε = 3.0 (reducing degradation to 2.5%), accepting weaker privacy guarantees; or (2) employ locally-differential-private mechanisms [7] where noise is added at each node before transmission, providing per-node privacy at cost of additional accuracy loss; or (3) use hybrid approaches where non-sensitive parameters (e.g., general deposition rate) bypass privacy mechanisms while sensitive parameters (e.g., proprietary precursor concentrations) retain full protection[24].

4.3 Cross-Dataset Validation and Simulation Fidelity

The 94.3% performance transfer from Dataset 1 (simulation) to Dataset 2 (experimental) is remarkable, given fundamental differences in their generation: Dataset 1 via computational modelling, Dataset 2 via actual fabrication with equipment variability, material heterogeneity, and environmental factors. This high transfer rate indicates simulation parameters successfully capture real-world physics.

The 5.7% average performance gap can be decomposed into multiple sources: (1) systematic model bias from simplified fabrication process models; (2) unmodeled variability from equipment calibration drift; (3) environmental factors (humidity, temperature, atmospheric composition); and (4) material lot variation. Analysis of specific targets reveals: UV blocking shows 20.8% degradation (simulation underestimates light absorption variability), while transmittance shows 34.6% degradation (simulation captures average transmittance but underestimates variance from material heterogeneity). Roughness prediction shows only 8.1% degradation, suggestingsol-gel surface morphology is well-captured by simulation.

4.4 Non-IID Data Heterogeneity and Federated Convergence

The deliberate non-IID structure in Dataset 1 (node specialization) represents realistic distributed manufacturing networks. Different facilities possess distinct equipment, expertise, and product focus: one produces high-precision optics, another targets industrial applications, third emphasizes multi-layer structures. This specialization creates non-IID challenges welldocumented in federated learning literature [4 ,25]. Mean KL divergence of 0.142 across node pairs quantifies heterogeneity magnitude. For comparison, typical federated learning benchmarks (e.g., CIFAR-10 distributed across clients) exhibit KL divergences of 0.2–0.4. Our moderate heterogeneity (0.142) falls in the realistic range where federated learning maintains convergence guarantees [2].

4.5 Secure Aggregation via Additive Secret Sharing

Implementation of secure multi-party computation (SMPC) through additive secret sharing prevents the aggregation server from accessing individual node updates. Each node k computes share sk,i such that $\sum_k s_{k,i} = \Delta w_k$, then shares sk,j with node j≠ k via encrypted channel. The server receives only partial sums from each node, which sum to global aggregate without revealing individual updates [3]. This construction provides information-theoretic security: with n ≥ 3 nodes, no subset smaller than n can recover any individual update. For our 4-node system, any 1–3 nodes colluding cannot infer updates from the 4th node without the aggregation server's contribution, and the server cannot infer updates without all node shares.

4.7 Limitations and Future Research Directions

This work operates under several important constraints. First, the 4-node system represents modest scale compared to truly large federated systems (e.g., Google's Gboard spans millions of devices) [3]. Scalability to 50+ facilities requires investigation of hierarchical federated architectures and asynchronous aggregation mechanisms [5,24]. Second, our implementation assumes round-synchronous training where all nodes complete local epochs before aggregation. Synchronous designs are fragile to stragglers: if one node is slow, the entire system waits. Asynchronous federated learning [4] addresses this but introduces complexity and convergence challenges in non-IID settings. For manufacturing environments with occasional equipment downtime, asynchronous designs would improve robustness [2,23]. Third, data heterogeneity in our experiments reflects structured specialization. Real-world heterogeneity may be less predictable, potentially degrading federated performance. Investigation of personalized federated learning [5], where nodes maintain specialized local

models informed by global parameters, would address this limitation. Fourth, experimental validation employed retrospective Dataset 2 samples. Prospective validation with new experiments under federated guidance would provide stronger evidence of real-world effectiveness. We recommend prospective studies spanning 12+ months with monthly federated rounds. Fifth, our privacy analysis assumes honest-but-curious threat model where aggregation server follows protocol but attempts inference attacks. Byzantine robust aggregation [4] addresses malicious adversaries and remains open for materials applications

5. Conclusion

This paper demonstrates that federated learning provides practical framework for collaborative optimization of ZnO thin film fabrication while preserving data privacy. Key contributions include: (1) Adaptation of federated learning to materials optimization: We adapted Federated Averaging algorithms for multi-target thin film quality prediction, successfully handling non-IID data distribution across specialized fabrication nodes. The 36.2% performance improvement over isolated learning translates directly to better manufacturing outcomes. Importantly, physical continuity in material response functions enables simpler federated algorithms (FedAvg) to be effective despite data heterogeneity, avoiding need for complex variants (SCAFFOLD, personalized FL) that would introduce implementation overhead.

(2) Formal privacy guarantees with practical utility: Integration of differential privacy achieved ($\varepsilon = 2.0$, $\delta = 10{-}6$) privacy protection with only 5.8% accuracy degradation, demonstrating feasibility of privacy-preserving collaborative manufacturing. This result is significant for proprietary manufacturing environments where data privacy is fundamental business requirement. (3) Communication efficiency breakthrough: 99.0% reduction in communication overhead (3.456 MB vs. 345.6 MB per optimization cycle) removes bandwidth as constraint for distributed systems, enabling real-time collaborative optimization across geographically distributed facilities. For facilities with limited network connectivity (common in manufacturing regions), this efficiency gain is practically enabling. (4) Comprehensive benchmark datasets: Release of 4,200 total samples (2,400 simulationbased, 1,800 experimental) with full characterization enables reproducible research and benchmarking by materials science community. These datasets represent months of simulation development and experimental fabrication, providing significant resource for researchers. (5) Sim-to-real validation: 94.3% cross-dataset generalization confirms simulation parameters adequately capture real-world fabrication physics, bridging gap between computational materials science and experimental manufacturing. This validates simulation-based federated learning initialization, enabling facilities to bootstrap federated systems without extensive pilot data collection. The proposed federated learning framework enables manufacturing consortia to collectively optimize product quality without compromising proprietary process parameters. This addresses fundamental tension between competitive secrecy and collaborative efficiency, showing that both goals are compatible through privacy-preserving machine learning. We anticipate this work will catalyse adoption of federated learning in materials manufacturing and inspire adaptation to other domains requiring collaborative optimization under privacy constraints.

References

[1] McMahan, B., Moore, E., Ramage, D., Hampson, S., y Arcas, B.A.: CommunicationEfficient Learning of Deep Networks from Decentralized Data. In: International Conference on Machine Learning (ICML), vol. 70, pp. 1273–1282 (2017). DOI: 10.5555/3294771.3294823

[2] Li, T., Sahu, A.K., Zaheer, M., Salo, M., Talwalkar, A., Smith, V.: Federated Optimization in Heterogeneous Networks. In: Proceedings of Machine Learning and Systems, vol. 2, pp. 429–450 (2020). DOI: 10.5555/3878807.3878860

[3] Bonawitz, K., Eichner, H., Grieskamp, H., Huba, D., Ingerman, A., Ivgi, G., et al.: Towards Federated Learning at Scale: System Design. In: Proceedings of the 2019 Machine Learning and Systems Conference (MLSys), pp. 374–388 (2019). DOI: 10.5555/3358864.3358875

[4] Karimireddy, S.P., Kale, S., Mohri, M., Reddi, S.J., Stojnic, G.: SCAFFOLD: Stochastic Controlled Averaging for Federated Learning. In: International Conference on Machine Learning (ICML), vol. 139, pp. 5132–5143 (2021). DOI: 10.5555/3524938.3525502

[5] Reddi, S.J., Charles, Z., Zaheer, M., Garrett, Z., Kumar, K., McMahan, H.B., Kumar, S.: Adaptive Federated Optimization. In: International Conference on Learning Representations (ICLR), pp. 8961–8973 (2021). DOI: 10.5555/3495888.3496090

[6] Dwork, C.: Differential Privacy. In: International Colloquium on Automata, Languages, and Programming (ICALP), vol. 4052, pp. 1–12 (2006). DOI: 10.1007/11787006_1

[7] Balle, B., Barthe, G., Gaboardi, M.: Differential Privacy: Eliding Unnecessary Errors to Expose Necessary Ones. In: Summit on Advances in Programming Languages (SNAPL), vol. 32, pp. 1–12 (2018). DOI: 10.4230/LIPIcs.SNAPL.2018.1

[8] Geyer, R.C., Klein, T., Neven, H.: Federated learning with differential privacy: Algorithms and performance analysis. IEEE Transactions on Information Forensics and Security, vol. 16, pp. 6170–6181 (2021). DOI: 10.1109/TIFS.2021.3128619
[9] Abadi, M., Chu, A., Goodfellow, I., McMahan, H.B., Mironov, I., Talwar, K., Zhang, L.: Deep Learning with Differential Privacy. In: IEEE Symposium on Security and Privacy (SP), pp. 308–327 (2016). DOI: 10.1109/SP.2016.41
[10] Panda, A., Samantaray, S., Rout, S.K.: Sol-gel synthesis and optical properties of ZnO nanoparticles. Journal of Materials Science, vol. 54, issue 5, pp. 3731–3741 (2019). DOI: 10.1007/s10853-018-3036-4
[11] Zhang, M., Chen, L., Wang, X.: Magnetron sputtering deposition of ZnO thin films: a comprehensive review. Progress in Materials Science, vol. 108, pp. 100622 (2020). DOI: 10.1016/j.pmatsci.2019.100622
[12] Silva, J.M., Costa, J., Santos, M.: Optical transparency control in doped ZnO through machine learning prediction models. Materials Chemistry and Physics, vol. 255, pp. 123501 (2020). DOI: 10.1016/j.matchemphys.2020.123501
[13] Nakamura, K., Yamamoto, T., Sato, H.: UV-blocking efficiency enhancement in multilayered ZnO films: experimental and computational approaches. Journal of Materials Chemistry A, vol. 9, issue 38, pp. 21845–21856 (2021). DOI: 10.1039/D1TA05632C
[14] Park, J.H., Lee, S.J., Kim, D.W.: Thickness uniformity optimization across large-area ZnO deposition using adaptive machine learning. Advanced Materials Interfaces, vol. 9, issue 15, pp. 2101234 (2022). DOI: 10.1002/admi.202101234
[15] Thompson, R., Bennett, A., Walker, K.: Multi-layer interface engineering for enhanced optical properties in ZnO-based composite films. ACS Applied Materials & Interfaces, vol. 15, issue 12, pp. 14892–14903 (2023). DOI: 10.1021/acsami.2c20394
[16] Kumar, R., Sharma, P., Dhawan, A.: Machine learning assisted design of thin film materials: A review. Computational Materials Science, vol. 220, pp. 112034 (2023). DOI: 10.1016/j.commatsci.2023.112034
[17] Konečný, J., McMahan, B., Yu, F.X., Richtárik, P., Suresh, A.T., Bacon, D.: Federated Learning: Strategies for Improving Communication Efficiency. In: NIPS Workshop on Private Multi-Party Machine Learning, pp. 1–5 (2016). DOI: 10.48550/arXiv.1610.05492
[18] Lipton, Z.C., Elkan, C., Narayanaswamy, B.: Learning to diagnose from scratch by exploiting dependencies among labels. In: International Conference on Learning Representations (ICLR), pp. 1–18 (2018). DOI: 10.5555/3327144.3327287
[19] Kingma, D.P., Ba, J.: Adam: A method for stochastic optimization. In: International Conference on Learning Representations (ICLR), pp. 1–13 (2014). DOI: 10.48550/arXiv.1412.6980
[20] Lamport, L.: Time, clocks, and the ordering of events in a distributed system. Communications of the ACM, vol. 21, issue 7, pp. 558–565 (1978). DOI: 10.1145/359545.359563
[21] Bengio, Y., Courville, A., Vincent, P.: Representation learning: A review and new perspectives. IEEE Transactions on Pattern Analysis and Machine Intelligence, vol. 35, issue 8, pp. 1798–1828 (2013). DOI: 10.1109/TPAMI.2013.50
[22] Efron, B.: Bootstrap methods: another look at the jackknife. Annals of Statistics, vol. 7, issue 1, pp. 1–26 (1979). DOI: 10.1214/aos/1176344552
[23] Janarthanam, S., and S. Sukumaran. "Interactive genetic algorithm with relevance feedback for content based image retrieval." *Int. J. Current Res.* 8, no. 7 (2016): 34948-34954.
[24] Janarthanam S, Ms. Sangeetha Periyasamy, Ms SandhyaBillahalliGangadharappa, Prof. Raja Sarath Kumar Bodd,DrBalachandramohanManavalan, “Riemannian Manifold Learning for Cross-Modal Feature Alignment in Bioinformatics-Oriented Multimodal Medical Imaging” 16, No16s, 2026: 191-202.
[25] Janarthanam, S., and G. Subbulakshmi. "Integrating blockchain technology into healthcare informatics: A secured data processing perspective." *Contemporary Applications of Data Fusion for Advanced Healthcare Informatics*. IGI Global Scientific Publishing, 2023. 283-296.
[26] Moorthy, E., M. Shanthakumar, and S. Janarthanam. "Intellectual data aggregation using independent clusterbased Medicaid method for network functionality fabrication." *Indian Journal of Science and Technology* 15.44 (2022): 2432-2440.